# LIMNOLOGY and OCEANOGRAPHY

# Prairie stream metabolism recovery varies based on antecedent hydrology across a stream network after a bank-full flood

Claire M. Ruffing,[1,a] Allison M. Veach [ID],[1*,b] Anne Schechner,[1] Janine Rüegg [ID],[1,c] Matt T. Trentman [ID],[1,d] Walter K. Dodds [ID][1]
[1]Division of Biology, Kansas State University, Manhattan, Kansas

## ABSTRACT

Intermittent streams are characterized by significant periods of low to no flow, yet are also frequently subjected to flashy, high floods. Floods alter ecosystem function and result in variable successional patterns across the stream network. Yet, the timing of restored function after floods in intermittent stream networks is relatively unexplored. We measured recovery of stream ecosystem function using rates of gross primary production (GPP), ecosystem respiration (ER), net ecosystem production (NEP), and the primary production to respiration ratio (P/R) across eight locations in the Kings Creek drainage basin with differing preflood conditions (previously dry [intermittent] or flowing [perennial]) over a 30-d period following a 2-yr return interval flood. We found that all metabolic rates (GPP, ER, NEP, P/R) varied primarily by time (days since flood) and antecedent flow, but not spatial network position (i.e., drainage area). Intermittent sites exhibited high rates of ER (0.17–3.33 g dissolved oxygen [DO] m$^{-2}$ d$^{-1}$) following rewetting compared to perennial sites (0.03–1.17 g DO m$^{-2}$ d$^{-1}$), while GPP, NEP, and P/R were slower to recover and varied less between sites of differing preflood conditions. Metabolic rates were not strongly influenced by other environmental conditions. A large proportion of variation was explained by the random effect of location. Our results suggest that metabolism is temporally asynchronous and highly heterogenous across intermittent watersheds and that antecedent hydrology (drying prior to rewetting) stimulates heterotrophic activity, likely dependent on terrestrially derived organic matter and nutrient subsidies.

Intermittent lotic ecosystems are defined by low flow and eventually periodic drying. They comprise approximately 30% of the total length of all river networks globally (Tooth 2000), and flow ceases for at least 1 d yr$^{-1}$ on 51–60% of the world's rivers (Messager et al. 2021). Furthermore, stream intermittency will likely become more widespread due to increased climate-change-induced drought and water abstraction (Larned et al. 2010;

*Correspondence: allison.veach@utsa.edu

[a]Present address: The Nature Conservancy in Oregon, Portland, Oregon
[b]Present address: Department of Integrative Biology, The University of Texas at San Antonio, San Antonio, Texas
[c]Present address: Interdisciplinary Center for Mountain Research, University of Lausanne, Lausanne, Switzerland
[d]Present address: O'Connor Center for the Rocky Mountain West, University of Montana, Missoula, Montana

Gudmundsson et al. 2021). The heterogeneous flow regime caused by drying can lead to a greater coupling of terrestrial-aquatic systems during drying-wetting phases (Leigh et al. 2016). After a dry period, the "first flush" or "pulse" of flow into intermittent streams can stimulate dissolved organic matter (DOM) mobilization (Corti and Datry 2012; Wohl et al. 2017) and rapid nutrient uptake in streambeds due to terrestrial supply and export (Palmer and Ruhi 2019). However, local environmental conditions which vary spatially across stream networks may also impact the storage, transport, and processing of carbon, particularly in intermittent streams (Rüegg et al. 2015; Bernal et al. 2019).

Hydrological variability (e.g., flow cessation, flooding) in intermittent streams causes spatiotemporal heterogeneity in both biotic and environmental parameters driving ecosystem processes, such as stream metabolism (Uehlinger and Naegeli 1998). Net ecosystem production (NEP) and the primary production to respiration ratio (P/R) represent the relative importance of inorganic carbon to organic matter fixation (gross primary productivity [GPP]) and organic matter consumption (ecosystem respiration [ER]) and thus serve as integrative metrics describing energy dynamics. Both GPP and ER are tightly

coupled to environmental conditions (Young et al. 2008). For example, light, temperature, flow, and nutrient availability fundamentally regulate GPP and ER (Mulholland et al. 2001; Bernot et al. 2010; Demars et al. 2011). However, flow is likely the most spatially and temporally variable out of all environmental drivers regulating metabolism (Poff et al. 1997; Poff and Zimmerman 2010). Extreme floods scour river beds which limit GPP and ER by removing primary producer and consumer biomass (Fisher et al. 1982; Uehlinger and Naegeli 1998; Francoeur and Biggs 2006). Low magnitude flooding may not remove biofilm from streambeds, but flood-induced decreases in water temperature, increases in turbidity, and pulses of organic matter and nutrients could still influence GPP and ER. Despite these known drivers, the magnitude of flow influence on stream metabolism is limited to only a few studies with long-term monitoring (Uehlinger 2000; Roberts et al. 2007; Summers et al. 2020) or synoptic flood sampling (Reisinger et al. 2017; Qasem et al. 2019) across a narrow spatial extent (but see - Mejia et al. 2019).

Grassland stream networks are model systems for studying disturbance ecology because of their characteristic frequent cycles of flooding and drought (Matthews 1988; Dodds et al. 2004), yet the consequences of floods on ecosystem metabolism have not been well studied in these intermittent ecosystems. Prairie streams are characterized by a seasonally dry and warm climate, resulting in widespread intermittency, flashy flow regimes, and frequent flooding depending on the frequency and magnitude of precipitation events (Costigan et al. 2015). Under baseflow conditions, prairie streams are associated with low rates of ER and greater rates of GPP (relative to ER) due to high light inputs and warm stream temperatures. Thus, rates of NEP in these systems are near or above zero and they are more autotrophic compared to streams of other biomes (Bernot et al. 2010). Dodds et al. (1996, 1996) demonstrated that patch-scale estimates of algal biomass and GPP recover within 2 weeks following a spate with rates being highly dependent on light availability. The recovery of ER following floods in intermittent streams is less clear but, ER can increase significantly after rewetting (sediments specifically; Schiller et al. 2019) or recover more slowly similar to GPP (Jones et al. 1995). These trends are likely dependent on environmental conditions that differ among ecosystems or by location within a catchment (Cook et al. 2015). Such effects likely depend on the degree of bed movement, alterations to the hyporheic zone, the quantity and quality of any remaining allochthonous material, and the readiness of heterotrophic bacteria to metabolize available organic matter after terrestrial transport (Allen et al. 2020). Understanding whole-ecosystem flood recovery requires the examination of spatially explicit metabolic patterns in a stream network given the physical and metabolic heterogeneity of prairie stream networks and that flooding facilitates hydrologic connectivity among reaches.

Here, we asked how stream metabolism recovers following a 2-yr return interval flood across an entire prairie stream network following extended drought. Our specific objectives were to (1) quantify rates of GPP, ER, NEP, and P/R following the flood across eight locations within the network (spanning headwaters to the mainstem of Kings Creek, Manhattan, Kansas, USA), (2) explain the roles of network position and stream size, as measured by drainage area, and preflood hydrologic conditions (hereafter referred to as "antecedent flow") in the trajectory of those rates, and (3) identify environmental factors that explain resulting metabolic trends. Based on other work in these systems (Dodds et al. 1996; Veach et al. 2016), we hypothesized that (1) GPP rates would steadily increase following the flood as algal biomass accrued. Contrary to GPP, ER would increase rapidly after water-return due to the initial pulse of allochthonous matter stimulating heterotrophic microbial activity. After this initial nutrient and water pulse, we hypothesized that the heterotrophic component of ER would decrease through time due to resource-limitation. Second, we hypothesized (2) that metabolism will vary based on drainage area due to several environmental variables, such as stream discharge, temperature, and PAR, which all shift along the stream continuum. Third, we hypothesized (3) previously dry sites would have lower GPP and ER rates relative to perennial sites following the flood. Intermittent sites have minimally active biofilms prior to flow therefore can require time for growth before they substantially contribute to whole-ecosystem metabolism relative to perennial sites. Finally, we hypothesized (4) that the rate of decrease in discharge to baseflow conditions after flooding would have the greatest impact on temporal patterns of GPP, ER, NEP, and P/R among sites.

## Methods

### Study sites

Study sites were located in Kings Creek at Konza Prairie Biological Station (KPBS), approximately 16 km south of Manhattan, Kansas (Fig. 1). The KPBS is a 3847-ha tallgrass prairie preserve located in the Flint Hills of northeastern Kansas, USA, and has served as a National Science Foundation (NSF) Long-Term Ecological Research (LTER) site since 1980. Typically, this region receives greater than 800 mm of precipitation annually, although interannual variability is high (Hayden 1998). Approximately, 75% of annual precipitation occurs in late spring and early summer (Hayden 1998). Streamflow is intermittent in the Kings Creek catchment with an average of 190 zero-flow days at the mainstem USGS gage (#06879650), and the number of zero-flow days generally increases as watershed size decreases (Costigan et al. 2015) except for spring-fed reaches in some upstream areas of the watershed. The vegetation in the area consists of native tall-grass prairie (Samson and Knopf 1994) with dominant grass species of big bluestem (*Andropogon gerardii*), little bluestem (*Schizachyrium scoparium*), Indian grass (*Sorghastrum nutans*), and switchgrass (*Panicum virgatum*), although riparian
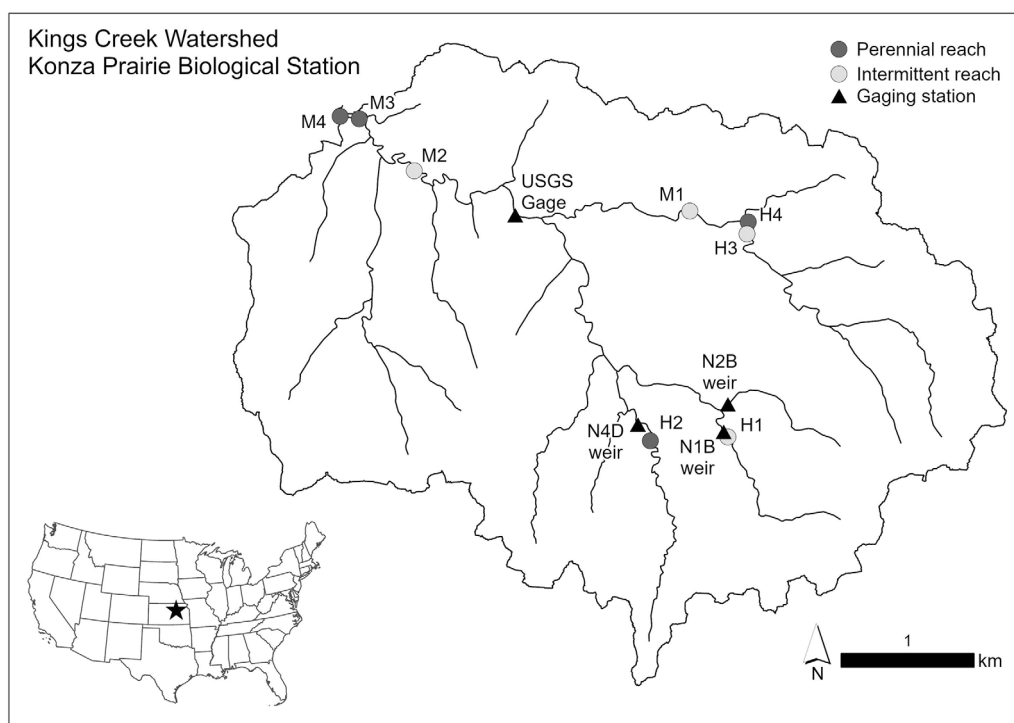
**Fig. 1.** Distribution of study reaches across the Kings Creek watershed at Konza Prairie Biological Station outside of Manhattan, Kansas (USA). Names of study reaches reflect their position in the network (H indicates headwater reaches, M indicates mainstem reaches, and numbers correspond to the increasing contribution to the watershed). Study reaches are denoted by circles and the USGS gaging station is denoted by a triangle. Perennial reaches are denoted in dark gray and intermittent, or dry, reaches are denoted by light gray circles. Discharge data used in this study was collected at the four gaging stations (three weirs and USGS gage, see Fig. 2).

woody expansion has occurred in most subwatersheds (Veach et al. 2014). Riparian areas along the study reaches presented here are dominated by grasses in the headwater reaches and mature gallery forest (notably, Bur oak [*Quercus macrocarpa*], Chinkapin oak [*Quercus muehlengergii*], Hackberry [*Celtis occidentalis*]) along the valley bottoms of the mainstem reaches.

### Environmental data collection

On 27 April 2014, KPBS and the surrounding area received approximately 70 mm of rain in 1 d (i.e., ~ 10% of annual average precipitation). Before this rainstorm, the area was experiencing multiyear drought conditions ranging from abnormally dry to extreme drought (data not shown). The USGS gage experienced 240 d of no flow prior to the flooding, and many headwater sites without springs experienced > 200 d without flow (Dodds 2020a,b,c,d). Peak flow (27,609 L s$^{-1}$ at USGS gage) occurred shortly after the rain started. This was a 2-yr return interval event based on the period of record for this gauge and moved considerable amounts of sediment and cobble in the stream channel. We established eight study reaches by 30 April 2014, within 3 d of the flood when flow had receded to 154 L s$^{-1}$ at the USGS gage (Table 1; Fig. 2). Four of the study sites were headwaters of the King's Creek network (H1–H4) and four were located along the mainstem (M1–M4; Fig. 1). Reaches H2, H4, M3,

and M4 maintain some degree of flow year-round while reaches H1, H3, M1, and M2 are intermittent and were dry prior to this flood.

We measured channel hydromorphology (width and depth), substrate size, and canopy cover for the upstream reach at each site (see Rüegg et al. 2016 for methodology; Table 2). In addition, we estimated daily discharge at all sites to assess the relative change in flow following the flood. Daily discharge for each site during the study period was estimated from the following regression equation ($p < 0.001$, adjusted $R^2 = 0.55$) developed for the Kings Creek watershed using discharge–area relationships and previously available data from three weirs located (Dodds 2020a,b,d) in headwaters and a USGS gage 06879650 on the mainstem of Kings Creek lower in the watershed.

$$Q = -2.08 + (0.7366 \times A) + (0.2743 \times \text{USGSQ}), \quad (1)$$

where $Q$ equals the discharge of a specific site (L s$^{-1}$), $A$ represents the contributing watershed area upstream of the corresponding site (km$^{-2}$) and USGSQ is the recorded daily discharge at the USGS gage converted to metric units (L s$^{-1}$). We recognize that this approach adds uncertainty to our estimates of discharge at each site; however, this relationship was our only way to estimate a time series of discharge at sites without gauges. Given the highly variable hydrology of the

**Table 1.** Site characteristics for the eight study reaches. Antecedent flow refers to flow characteristics at each reach before the flood; intermittent reaches were dry prior to the rain event while perennial retained some flow. Width and depth were collected synoptically after the flood and therefore do not represent the maximum flow conditions immediately following the flood. Substrate size is broken down as the median particle size ($D_{50}$) and the $16^{th}$ ($D_{16}$) and $84^{th}$ ($D_{84}$) percentiles. Average daily discharge reflects the entire 35 d after the flood and was estimated using Eq. 1 with numbers in parentheses being minimum and maximum daily flow.

| Site | Latitude | Longitude | Order* | Antecedent flow | Width (m) | Depth (cm) | Drainage area (km²) | Mean daily discharge (L s⁻¹) | Substrate size (mm) | | | Canopy cover (%) |
|---|---|---|---|---|---|---|---|---|---|---|---|---|
| | | | | | | | | | $D_{50}$ | $D_{16}$ | $D_{84}$ | |
| H1 | 39.09 | −96.59 | 1 | Intermittent | 1.6 | 13.3 | 1.1 | 10.6 (0–41.0) | 32 | 22 | 64 | 18.1 |
| H2 | 39.08 | −96.58 | 1 | Perennial | 1.8 | 10.0 | 1.2 | 10.7 (0.1–41.1) | 19 | 12.5 | 22.6 | 27.2 |
| H3 | 39.10 | −96.57 | 2 | Intermittent | 2.5 | 8.0 | 2.6 | 11.7 (1.1–25.0) | Na† | Na† | Na† | 82.7 |
| H4 | 39.10 | −96.57 | 2 | Perennial | 2.7 | 5.9 | 2.6 | 11.7 (1.1–42.1) | 32 | 22.6 | 738.4 | 57.4 |
| M1 | 39.10 | −96.58 | 2 | Intermittent | 3.6 | 4.5 | 3.7 | 12.5 (1.9–42.9) | 32 | 25.4 | 48.8 | 82.3 |
| M2 | 39.10 | −96.60 | 3 | Intermittent | 2.7 | 6.7 | 13.0 | 19.4 (8.8–49.8) | 11 | 5.0 | 20.6 | 88.0 |
| M3 | 39.10 | −96.61 | 4 | Perennial | 3.6 | 8.4 | 17.1 | 22.4 (11.8–52.8) | 32 | 0.002–0.05‡ | 52.3 | 61.8 |
| M4 | 39.10 | −96.61 | 4 | Perennial | 3.6 | 9.4 | 17.1 | 22.4 (11.8–52.8) | 23 | 8.7 | 63 | 47.5 |

*Order depends on flow conditions. When the whole network is flowing, as it was following the flood, Lower Kings Creek is a $4^{th}$ order stream.

†H3 was scoured down to bedrock following the flood.
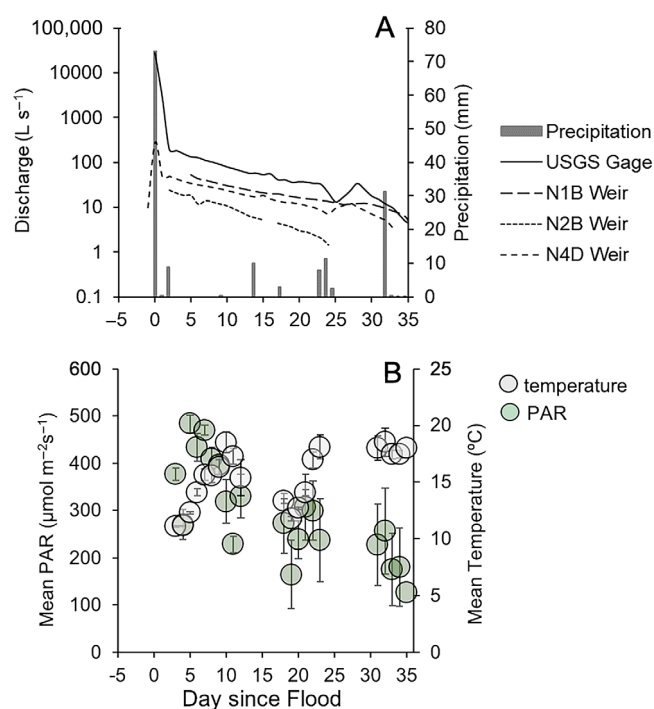
‡indicative of silt.



**Fig. 2.** Daily discharge (L s⁻¹), daily precipitation (mm; **A**), mean daily PAR (green circles) and mean daily temperature (**B**; gray circles) for the Kings Creek watershed during the study period. Discharge was measured at the Kings Creek USGS gaging station (06879650) for the entirety of the study and intermittently at three headwater weirs operated by KPBS. Precipitation data is from the meteorological station also operated by KPBS. Day 0 corresponds to 27 April 2014, the day the flood occurred. Discharge values are plotted on a log scale for clarity and the traces stop when the channel dried. PAR and temperature data points represent the mean among sites for each day with metabolism data.

site, it is not surprising that we did not have greater statistical power to explain variance. However, the equation was based on stations that covered over half of the area of the total watershed, so provides representative indications of flow. Still, our results should be considered cautiously based on the highly temporal and spatial variation in the system (Schechner et al. 2021). We have high certainty of the spring fed areas that were permanent upstream as we had been sampling these sites during the extended drought.

## Metabolism data collection

We used data loggers to record values of dissolved oxygen (DO), temperature, and barometric pressure for multiple days at a time (YSI ProODO data loggers with custom extended battery pack, Yellow Springs Instruments). Photosynthetically active radiation (PAR) was logged with Odyssey integrating PAR sensors (Dataflow Systems PTY Limited). Both sensors were deployed in the thalweg of the stream at each site and set to log continuously at 10-min intervals. Data loggers were calibrated in the lab or field prior to and following deployment (Schechner et al. 2021) and were monitored in the field for approximately 35 d with at least weekly site visits and

**Table 2.** Statistical summary of stream metabolism estimates at each site (expressed in g $O_2$ m$^{-2}$ d$^{-1}$). GPP and ER (reported as a positive value to indicate consumption) were modeled using the BASE method (Grace et al. 2015; Song et al. 2016) and presented as mean and range (min–max) over the days recorded as well as the coefficient of variation among the days of each site. Rates for NEP show the difference between GPP and ER (i.e., negative = net heterotrophic).

| Site | Days modeled | GPP Mean (min-max) | CV | \|ER\| Mean (min-max) | CV | NEP Mean (min-max) | CV | P/R Mean (min-max) | CV | $K_{DO}$ (day$^{-1}$) Median (min-max) |
|------|------|------|------|------|------|------|------|------|------|------|
| H1 | 6 | 0.66 (0.13–1.10) | 63.44 | 3.35 (2.75–4.14) | 16.45 | −2.69 (−3.34 – −2.12) | 15.18 | 0.19 (0.04–0.32) | 0.62 | 17.49 (7.17–37.75) |
| H2 | 17 | 0.44 (0.21–0.82) | 33.10 | 0.68 (0.08–1.44) | 58.28 | −0.25 (−1.13–0.25) | 169.65 | 1.03 (0.17–3.14) | 0.81 | 37.34 (10.59–39.63) |
| H3 | 5 | 0.35 (0.29–0.41) | 14.43 | 3.32 (3.20–3.50) | 3.49 | −2.97 (−3.09 – −2.80) | 3.69 | 0.11 (0.09–0.12) | 0.14 | 26.54 (19.00–30.95) |
| H4 | 14 | 0.04 (0.00–0.08) | 66.96 | 0.26 (0.07–0.45) | 47.08 | −0.22 (−0.45 – −0.03) | 64.64 | 0.23 (0.01–0.60) | 0.99 | 6.00 (3.01–37.27) |
| M1 | 19 | 0.04 (0.00–0.09) | 70.42 | 0.48 (0.20–0.70) | 33.25 | −0.44 (−0.64 – −0.17) | 34.69 | 0.09 (0.00–0.18) | 0.68 | 14.00 (0.00–38.88) |
| M2 | 17 | 0.18 (0.00–0.42) | 81.93 | 0.71 (0.27–1.01) | 25.36 | −0.54 (−0.69 – −0.20) | 23.35 | 0.23 (0.00–0.49) | 0.70 | 12.85 (8.36–34.96) |
| M3 | 14 | 0.30 (0.00–0.58) | 73.67 | 0.49 (0.36–0.67) | 17.80 | −0.19 (−0.47–0.07) | 95.19 | 0.58 (0.00–1.21) | 0.73 | 6.83 (5.27–16.77) |
| M4 | 14 | 0.31 (0.00–0.67) | 76.95 | 0.49 (0.40–0.77) | 23.39 | −0.18 (−0.47–0.11) | 102.35 | 0.59 (0.00–1.27) | 0.75 | 7.24 (5.31–10.63) |

calibration checks. Technical difficulties due to battery failure, sensor malfunction, and destructive activity by rodents prevented continuous data collection at some sites. Newly calibrated replacement sensors were deployed as soon as was logistically feasible.

### Metabolism modeling

Rates of GPP and ER were determined based on measurements following the single station open-system technique (Odum 1956) to track the trajectory of change in metabolism following the storm event at each site. NEP was calculated as the difference between GPP and ER. Rates were modeled using the modified Bayesian Single-station Estimation (BASE) model (v2.3 Grace et al. 2015; Song et al. 2016). This method is an extension of the daytime regression model (Kosinski 1984) where GPP and ER are modeled as

$$[DO]_{t+1} = [DO]_t + AI_t^p - R\left(\theta^{(T_t-T)}\right) + K_{DO} \times \left(1.0241^{T_t-T}\right) \times \left([DO]_{sat,t} - [DO]_{modelled,t}\right), \qquad (2)$$

where $t$ is the timestep; $AI^p$ is the term for primary production (mg $O_2$ L$^{-1}$ d$^{-1}$) where $A$ is a constant, $I$ is incident light intensity, and $p$ is an exponent for photo-saturation; $R$ is respiration (mg $O_2$ L$^{-1}$ d$^{-1}$); $\theta$ is the temperature dependence of respiration; $T_t$ and $T$ are water temperature at time $t$ and average daily water temperature, respectively; $K_{DO}$ is the aeration coefficient (d$^{-1}$); and subscripts "sat" and "modeled" refer to [DO] at either saturation or modeled concentrations. We set $\theta$ equal to 1.045 (Parkhill and Gulliver 1999), $p$ equal to 1.0, and used fixed values of $K_{DO}$, as described below, to model GPP and ER for every day that had continuously logged DO, temperature, and PAR over the 24-h period starting at 12 am. Each 24-h dataset with 10-min intervals was run with 20,000 modeled iterations, half of which were burn-in iterations in accordance with the model defaults. When Markov Chain Monte Carlo (MCMC) estimations did not converge in the modeling output, we increased runs to 50,000 iterations to improve model fit. Model output was converted from mg $O_2$ L$^{-1}$ d$^{-1}$ to g $O_2$ m$^{-2}$ d$^{-1}$ using average depth at each site surveys (data derived from Rüegg et al. 2016).

Due to breaking the data into 24-h periods (which was necessary given the relatively rapid changes in discharge), some models were poorly constrained with great variation in predicted values for $K_{DO}$ among days (Supporting Information Fig. S1), which resulted in correlation between $K_{DO}$ and ER (data not shown); therefore, we used the following approach to address these problems. We know from prior direct measures of aeration in this watershed using tracer gasses (data not shown) that large fluctuations in $K_{DO}$ do not occur during normal flow conditions, and that $K_{DO}$ can modestly increase, decrease, or remain relatively constant with changes in discharge at a particular site depending upon channel morphology. Therefore, in the absence of direct measures of $K_{DO}$ for

every day at every site, we ran an initial set of BASE models for each day at every site (which started 3 d postflood) where the model predicted values of $K_{DO}$. The median value of $K_{DO}$ for each site was then used as a fixed value for a second modeling run to generate the final dataset of metabolic rates at each site for each day (Table 2; Supporting Information Fig. S2). This approach resulted in more conservative estimates of $K_{DO}$ and removed the correlation with ER. We acknowledge that an approach exists which links discharge to gas exchange in hierarchical Bayesian metabolism models (Appling et al. 2018); however, this approach is less effective with short-term datasets.

**Statistical analysis**

We used linear mixed effects (LME) models to test (1) whether location within the stream network as determined by drainage area or hydrologic conditions prior to flooding (wet, dry) influenced the temporal pattern in daily rates of GPP, ER, NEP, and P/R following the flood and (2) whether light, stream temperature, or discharge explained the variation in rates across the network. Linear mixed effect models with maximum likelihood estimation (method = ML) were calculated and included two approaches. In the first approach, to test for effects of recovery across the network, the fixed covariates were days since flood (continuous), drainage area (continuous), and the antecedent flow (categorical: wet or dry) with the above-mentioned metabolism metrics as dependent variables. We think that wet vs. dry adequately captured the number of antecedent dry days since the 4 continuously monitored sites at various intermittent locations in the watershed had slightly more than 200 dry days prior to the flood. The interaction terms included day since flood × drainage area and day since flood × antecedent flow. In the second approach, to test for environmental drivers of metabolism after the flood, mean daily PAR, mean daily temperature, and estimated daily discharge were included as fixed covariates for GPP, ER, NEP, and P/R (dependent variables). Based on previous findings of the importance of autotrophic production throughout prairie stream networks (Dodds et al. 1996), and the fact that

autotrophs respire, we also included GPP as a predictor variable for ER. Site was included as a random effect in all LME models and an autocorrelation structure (AR(1)) was also included to allow variance to change across days in the second approach (Zuur et al. 2009). We used Akaike's information criterion (AIC) to select the most parsimonious model for each rate.

We also used multiple linear regression models (MLR) to test whether drainage area, antecedent flow conditions, in conjunction with continuous, environmental characteristics (average discharge, temperature, and PAR) explained the CV in GPP, ER, and NEP at each site since there was not enough statistical power to test complex model structures. The mean of environmental characteristics within a site over time were calculated to run the MLR models. All statistical analyses were performed in RStudio Version 1.0.136 (R Core Team 2019 version 3.6.1) using the base stats package for simple linear regression models, the lme4 package (Bates et al. 2015) for the linear mixed effects models, and the MuMIn package (Barton 2009) for calculating the model fit ($R^2$ marginal and $R^2$ conditional) of the mixed effects models.

## Results

**Spatiotemporal patterns in stream metabolism**

Stream metabolism varied across sites (Table 2) and much of this variation spatially was attributed to antecedent flow conditions (dry, perennial; Table 3). Rates also exhibited strong temporal trends (Fig. 3; Supporting Information Figs. S3, S4), which were largely influenced by antecedent flow conditions (Table 3). GPP rates ranged from 0.04 to 0.66 g $O_2$ $m^{-2}$ $d^{-1}$ and ER ranged from 0.26 to 3.35 g $O_2$ $m^{-2}$ $d^{-1}$ across sites (Fig. 3; Table 2). Previously dry sites had increases in GPP after flooding from 0.06 to 0.54 g $O_2$ $m^{-2}$ $d^{-1}$ and then declined at 22 d postflood (mean GPP among dry sites: 0.09 g $O_2$ $m^{-2}$ $d^{-1}$) and maintained low rates until the end of the study (Fig. 3A). At perennial sites, GPP increased similarly but at a faster rate postflood from 0.08 to 0.57 g $O_2$ $m^{-2}$ $d^{-1}$ at day 23. At the end of the study (35 d), both perennial and dry

**Table 3.** The best performing model from linear mixed effect models testing whether days since flooding (day), drainage area (DA) or antecedent flow conditions (AF) explained the pattern in rates of GPP, ER, NEP, and the ratio of GPP to ER (P/R). Site was included as a random effect in all models. The day since flood (continuous), drainage area, and antecedent flow (i.e., flowing or dry) were included as fixed effects. Model performance metrics include AIC, the variance explained by the fixed portion(s) of the model ($R^2_{fixed}$), the variance explained by the random portion(s) of the model ($R^2_{random}$), and the variance explained by the fixed and random components of the model ($R^2_{cond}$). Asterisks (*) denote model parameters that were significant ($p < 0.05$) and dashes denote parameters that were not included in the top model.

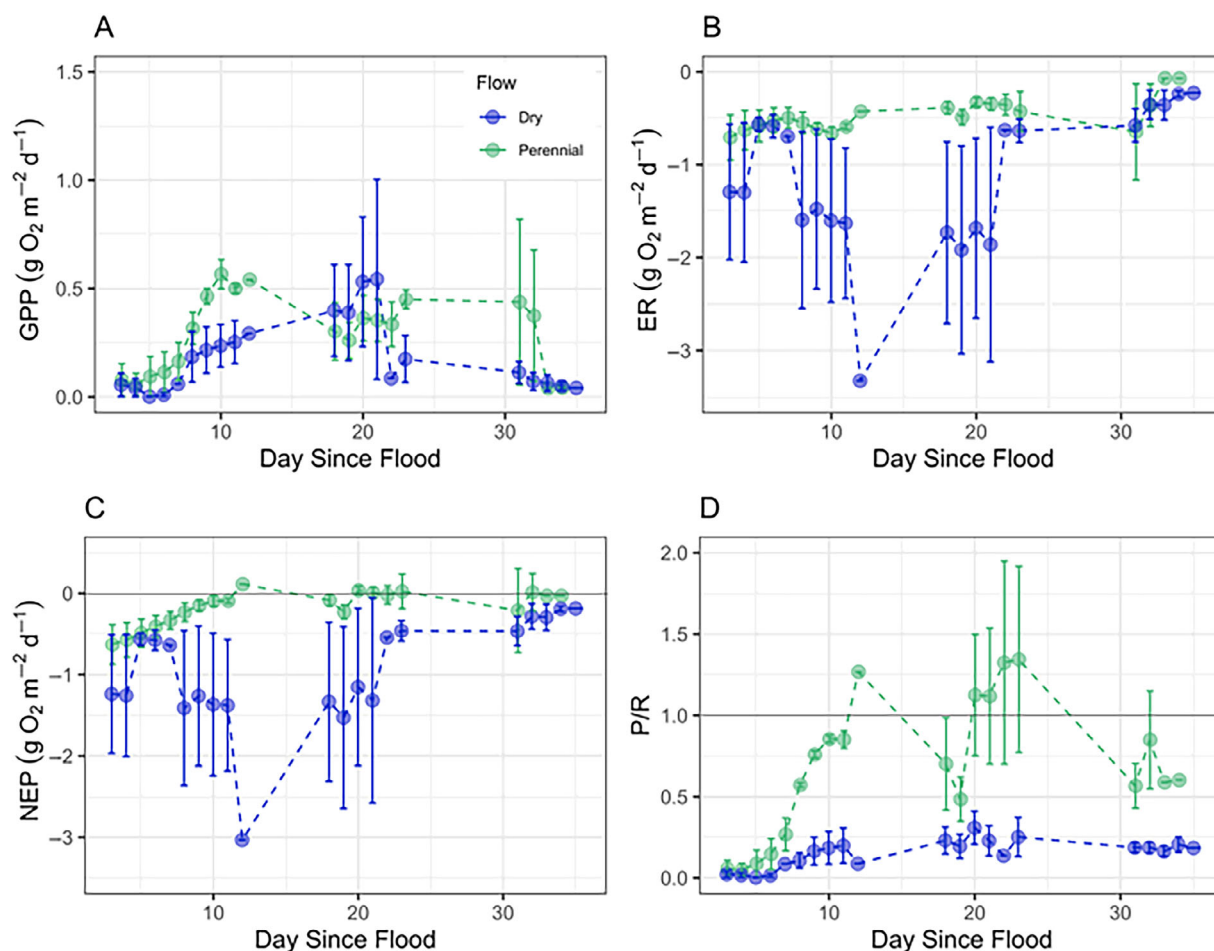| Model | Intercept | Day | DA | AF | Day × DA | Day × AF | AIC | $R^2_{fixed}$ | $R^2_{random}$ | $R^2_{cond}$ |
|---|---|---|---|---|---|---|---|---|---|---|
| GPP ~ intercept + day | 0.17* | 0.01* | — | — | — | — | −59.8 | 0.08 | 0.57 | 0.65 |
| ER ~ intercept + day + AF | 2.06* | −0.01* | — | −1.48* | — | — | 41.6 | 0.36 | 0.61 | 0.97 |
| NEP ~ intercept + (day × AF) | −1.78* | 0.01* | — | 1.28 | — | 0.01* | −0.4 | 0.43 | 0.54 | 0.97 |
| P : R ~ intercept + (day × AF) | 0.07 | 0.01 | — | 0.02 | — | 0.03* | 93.0 | 0.41 | 0.20 | 0.61 |

**Fig. 3.** Mean GPP (**A**), ER (**B**), NEP (**C**), and P/R ratio (**D**) with standard error bars for dry and perennial sites over days since the flooding event on Konza Prairie Biological Station near Manhattan, Kansas. Dry antecedent flow conditions are shown in blue and sites flowing prior to flooding are shown in green. The blue and green dashed lines are meant to aid in the interpretation of changes through time. Black dashed lines are present for NEP and P/R to denote state change from heterotrophy to autotrophy. Time points with one replicate do not have SE bars.

sites had low GPP (mean among sites: 0.04 g $O_2$ m$^{-2}$ d$^{-1}$; Fig. 3A). ER was high immediately after the flood, responding faster than GPP, and rates were especially high for previously dry (mean among dry sites: 1.29 g $O_2$ m$^{-2}$ d$^{-1}$) relative to perennial sites (mean 0.70 g $O_2$ m$^{-2}$ d$^{-1}$ ER; Fig. 3B). Over time, perennial sites decreased in ER rates, down to a mean rate of 0.22 g $O_2$ m$^{-2}$ d$^{-1}$ by day 35. At previously dry sites, ER rates, though highly variable, generally increased overtime until 22 d postflood (mean among dry sites: 0.63 g $O_2$ m$^{-2}$ d$^{-1}$ ER) before decreasing until the end of the study period (mean among dry sites: 0.23 g $O_2$ m$^{-2}$ d$^{-1}$ at day 35; Fig. 3B). Differences in ER between dry and perennial sites affected NEP rate changes over time after flooding. Dry and perennial sites were net heterotrophic immediately postflood (mean NEP −1.24 and −0.63 g $O_2$ m$^{-2}$ d$^{-1}$, respectively), yet perennial sites shifted to net autotrophy by day 12, though barely (mean NEP 0.11 g $O_2$ m$^{-2}$ d$^{-1}$; Fig. 3C). Perennial sites maintained net autotrophy except for some time points after day 12 (days 16–18, day 31). Dry sites were highly net

heterotrophic throughout the study period until day 30 postflood and thereafter, when they approached a NEP of zero (mean −0.19 g $O_2$ m$^{-2}$ d$^{-1}$; Fig. 3C). Likewise, P/R was close to 0.25, indicative of heterotrophy, for dry sites throughout the study period, whereas perennial sites exceeded P/R of 1 several instances throughout the study period (Fig. 3D).

Factors influencing stream metabolism were similar across the Kings Creek network. Fixed effects of both days since flood and antecedent flow impacted ER, NEP, and P/R ratios, whereas GPP was only impacted by days since flood (Table 3). For GPP, ER, and NEP, the random effect of site ($R^2_{random} > 0.50$) accounted for more variation relative to fixed effects. By contrast, P/R ratios had more variation due to the fixed effect of the day and antecedent flow interaction ($R^2_{fixed} = 0.41$) relative to random effect (Table 3). Only temporal variation in ER, as measured by its CV, was weakly explained by antecedent flow conditions ($T = 2.53$, $p = 0.06$; full model: $p = 0.08$, Adj. $R^2 = 0.62$). No other metabolism rate CV correlated with antecedent flow or drainage area.

**Table 4.** The best performing model from linear mixed models testing the effects of environmental drivers on GPP, ER, NEP, and the ratio of GPP to ER (P/R). Site was included as a random effect in all models. Independent drivers tested include PAR, average daily temperature (temp,°C), average daily discharge ($Q$, L s$^{-1}$), and GPP (for ER only). Model performance metrics include AIC, the variance explained by the fixed portion(s) of the model ($R^2_{\text{fixed}}$), the random portion(s) of the model ($R^2_{\text{random}}$), and the variance explained by the fixed and random components of the model ($R^2_{\text{cond}}$). Asterisks (*) denote model parameters that were significant ($p < 0.05$) and dashes denote parameters that were not included in the top models.

| Model | Intercept | PAR | Temp | Q | GPP | AICc | ΔAICc | $R^2_{\text{fixed}}$ | $R^2_{\text{random}}$ | $R^2_{\text{cond}}$ |
|---|---|---|---|---|---|---|---|---|---|---|
| GPP ~ intercept + temp | −0.05 | — | 0.02* | — | NA | −191.1 | 0 | 0.05 | 0.0 | 0.05 |
| ER ~ intercept + $Q$ + PAR + GPP | 1.0* | < 0.01* | — | 0.14* | 0.53* | −48.0 | 0 | 0.02 | 0.94 | 0.96 |
| NEP ~ intercept + temp + PAR + Q | −1.16* | < 0.01 | 0.02 | −0.15* | NA | −45.2 | 0 | 0.02 | 0.94 | 0.96 |
| P : R ~ intercept + temp + PAR | −0.72* | < 0.01* | 0.06* | — | NA | 26.4 | 0 | 0.18 | 0.02 | 0.20 |

### Environmental drivers

PAR increased over time, whereas water temperature did not show strong temporal trends. Stream discharge declined over time (Fig. 2). All environmental drivers measured (PAR, water temperature, $Q$) influenced GPP, ER, NEP, or P/R ratios. Water temperature was a significant predictor for GPP and P/R ratios: both increased with increasing temperature. Average discharge was a significant predictor for ER and NEP: ER increased with discharge, whereas NEP decreased with increasing discharge. Mean PAR predicted ER and P/R ratios. For both, increasing PAR resulted in a decline in ER and P/R. The random site effect accounted for a much greater proportion of the variation for ER and NEP ($R^2_{\text{random}} = 0.94$) relative to the environmental predictors, whereas environmental predictors explained more variation for GPP ($R^2_{\text{random}} = 0.05$) and P/R ($R^2_{\text{random}} = 0.18$; Table 4). There were no significant relationships between average discharge, PAR, and water temperature and the CV of GPP, ER, NEP, or P/R ratios.

### Discussion

We measured stream metabolism for more than 30 d across an intermittent stream network following a 2-yr return interval flood to determine trajectories of function in relation to network position and preflood hydrological conditions. Partially in support of our hypothesis, GPP generally increased across sites following the flood and correlated with days since flooding. However, ER was more variable among reaches over time for previously dry sites. ER was high within 3 d after the initial water pulse in sites that were dry prior to the flood and showed similar increases over time as GPP in sites that were previously flowing. These trends suggest that the presence or absence of water prior to flow return determines trajectories of carbon mineralization rates in these systems. Interestingly, environmental variables did not explain ER and NEP, which were dependent on random site variation, whereas GPP was also not strongly influenced by the environment, with no variation explained by site. Our results indicate that spatiotemporal patterns in metabolism are partially determined by historical hydrological conditions and high ER in intermittent stream may increase overall heterotrophy in the network. Likewise, GPP was more driven by time since flooding and not environmental nor location-specific factors.

### Stream metabolism recovery

Flood recovery in streams depends on multiple factors related to stream size, prior flow conditions, and local, reach-scale characteristics (Mejia et al. 2019). Our data demonstrate that site accounts for a large amount of variation in GPP and ER. Specifically, GPP was greater overall in perennial reaches and ER and NEP exhibited higher rates in previously dry reaches. Time was also influential for all metabolic rates, although less so than antecedent flow conditions, particularly for ER and NEP. We hypothesized a pulse in ER related to flow-induced organic matter subsidies followed by a quick return to preflood rates, especially in the perennial sites, but did not see this consistently. The greatest rates occurred over several weeks with a modest ER pulse over the first few days. In contrast, Acuna et al. (2004) demonstrated that over a ~ 2-yr period, benthic organic matter accumulation accounted for much of the temporal variation in ER.

Temporal trends in GPP indicate that primary production is responsive to flooding among sites due to a "reset" after a flow disturbance. Other studies spanning larger rivers in Australia (Cook et al. 2015), alpine rivers (Uehlinger 2000), and urban streams (Qasem et al. 2019) show that GPP increases over time after flooding and is more sensitive to high velocity flows or bed-moving spates than ER (Uehlinger 2000). Our data support the idea that flooding, even of smaller magnitudes, resets autotrophic processes due to potential streambed scouring and results in stream ecosystem dependence on terrestrial subsidies, as evidenced by high ER, until algal biomass recovers. We did not observe any strong response in GPP or ER to the several less intense spates that occurred during the study period. This was demonstrated by low predictive relationships with stream discharge, and may be due to limitation of organic matter in the short timeframe between these spates (Seybold and McGlynn 2018). Other studies have demonstrated that even small magnitude flow events can reduce metabolism rates (Uehlinger 2006; Roberts et al. 2007) yet

many temporal studies have not been performed in flow-disconnected lotic ecosystems. Given some similarities in the temporal trends for many of our sites, despite spatial variation in mean rates, significant floods may be necessary to cause a system "reset" and metabolism recovery to occur in a drought-prone stream network. Additional studies are needed to elucidate this hypothesis by expanding stream ecosystem ecology in intermittent and ephemeral streams (Allen et al. 2020).

Our data do suggest that classical successional theory needs to be revamped with respect to stream metabolism, particularly where extremes of flooding and drying occur regularly. For example, Vitousek and Reiners (1975) suggest nutrient retention will follow biomass accrual during succession, but their idea is mostly based on forests where standing biomass is high and has little consideration of belowground carbon and metabolic activity. In this sense, streams vary from classical models as GPP is often limited to a thin, highly active biofilm on lighted surfaces, but ER is a function of deeper sediment storage which may be less influenced by disturbance, yet nonetheless play important biogeochemical roles (e.g., in nutrient uptake; Grimm 1987). The Vitousek and Reiners (1975) model may apply to stream metabolic properties mediated by terrestrial successional stage (Valett et al. 2002), but less theory has been developed around succession within the stream channel (but see Fisher et al. 1982; Grimm 1987). In addition, such models assume an extended period of recovery after disturbance, and intermittent streams in particular may be in a perpetual state of disequilibrium.

We do have some specific indications that succession in streams can occur despite this disequilibrium. Stream biofilm studies do suggest that community structure changes over successional time and that this could influence ecosystem metabolism due to physiological differences of dominant taxa within successional stages (Besemer et al. 2007; Passy and Larson 2011). Furthermore, studies of temporal patterns of colonization following wetting in Kings Creek indicate that grazer effects on biofilms may be more pronounced multiple weeks postdisturbance (Murdock et al. 2010), which may explain the decline in GPP toward the end of measurements in this study. Still, a conceptual framework of stream metabolic succession as influenced by hydrologic variance and biomes that streams are embedded in has not been well developed (Dodds et al. 2015) and may require consideration of contingencies of specific streams. For example, our intermittent stream network has variable rates of recolonization of animals based on position in the network (Fritz and Dodds 2005), and this contingency could cause the temporal trajectory of metabolism to vary from streams which are more connected prior to disturbance.

### Antecedent flow conditions and stream microbial activity

Flow conditions prior to this flood event influenced whole-ecosystem NEP largely due to high rates of ER in previously dry locations. This effect is partially due to algal recovery dynamics (Frost et al. 2007; Battin et al. 2016) where algae require a significant recovery period once flow resumes compared to heterotrophic microorganisms. Algal communities are sensitive to low water availability and desiccation therefore drying in stream beds causes mortality and declines in biomass (Timoner et al. 2012). By comparison, most groups of bacteria are desiccation tolerant, depending on humidity of underlying sediments (McKew et al. 2011; Sabater et al. 2016), or can undergo metabolic dormancy (Lennon and Jones 2011) until water returns. We posit that large ER rates in previously dry sites is due to stimulatory response of freshwater bacteria to (1) terrestrial export and presence of dissolved organic carbon and other nutrients being released from soil aggregates, immediately after the flood pulse (Rüegg et al. 2015) that stimulates ER (Demars 2019) and (2) additional nutrient pulses resulting from lysing of within-stream microbial biomass and necromass (poor osmoregulation to extreme changes in water availability) which is a commonly documented occurrence in dry bulk soils after a rewetting event (Fierer & Schimel 2002; Schimel et al. 2018). This "Birch effect" would partially explain the high ER rates found immediately after rewet, similarly documented for soils (Salazar et al. 2018) and the eventual reduction in ER over time. Contrary to algae which require wet conditions, bacteria are generally ubiquitous regardless of water availability (Battin et al. 2016), can maintain cellular viability during droughts, as demonstrated for soils in this biome (Zeglin et al. 2013) and will metabolize available nutrients immediately upon rewetting due to their overall drought tolerance relative to other stream microbiota. Together, these processes may stimulate microbial respiration when antecedent conditions are dry relative to baseflow unlike primary production which requires algal recruitment and growth to occur before rates recover.

### Spatial heterogeneity and environmental correlates of ecosystem metabolism

We expected spatial heterogeneity in rates of GPP and NEP across the Kings Creek network. Specifically, with headwaters exhibiting greater net autotrophy and mainstem sites having greater net heterotrophy due to the differences in riparian vegetation. This hypothesis was not supported. Grasses and shrubs typically dominate the land cover in prairie ecosystems. However, in recent decades riparian grasslands have shifted to mature gallery forests at Konza Prairie, especially along the riparian corridors of perennial, mainstem stream reaches (Veach et al. 2014; Larson et al. 2019). Riley and Dodds (2013) manipulated riparian forest canopy cover and found that GPP and ER variation was tied to seasonal leaf loss and canopy presence. Canopy cover did not explain any variation in stream metabolism, which may be due to light levels not reaching the threshold for effects on NEP as has been found in other studies in the Kings Creek watershed (Dodds et al. 1996, Trentman et al. 2020). Regardless, the presence of large random site-level variation suggests there are drivers we

did not account for (site or reach-specific variables; Yates et al. 2018). In the Kings Creek watershed, there is high reach-scale variability in organic matter quality (Farrell et al. 2018) and quantity due to riparian vegetation, geomorphology, and proximity to spring seeps (Rüegg et al. 2015), which may ultimately change heterotrophic activity and algal accrual (Frost et al. 2007). We did find that ER was highly variable among sites, potentially related to environmental factors we did not measure in this study, such as geomorphology, and these factors could mask some temporal responses of stream metabolism. Metabolic rates at perennial sites had similar magnitudes and temporal patterns. Intermittent sites, independent of network position, were almost three times more variable over time in NEP than perennial reaches. This could indicate that intermittent reaches within this stream network may respond to flow events asynchronously or randomly (Mejia et al. 2019) due to large variability that was demonstrated in metabolism. Our results further suggest that channel networks that support extensive intermittent reaches may show greater overall metabolic variability than those more dominated by perennial flow.

We originally hypothesized that discharge would be the primary environmental driver explaining trends in metabolic rates, but this was not supported for GPP or ER. The results of our linear mixed effects models suggest that the decreasing discharge and increasing water temperature may be acting in concert to influence rates of ER and NEP. Some of the variation unaccounted for by environmental drivers may be due to network patchiness in organic matter availability in relation to floods. Trentman et al. (2020) found that postflood measurements of fine benthic organic matter (FBOM) at a subset of these study sites were substantially lower in a mainstem reach with permanent flow (site M4). Minimal flushing of organic matter in dry headwater sites, likely due to lower discharge relative to mainstem sites, may support resiliency and fuel ER postflood, given that in the same study FBOM explained a large amount of variation in ER estimates (Trentman et al. 2020). Furthermore, microbial responses to drying-rewetting may also dictate heterotrophic activity immediately after flow returns (Schimel 2018). We postulate that organic matter quantity and quality are likely ultimate drivers of metabolic trends although the proximate controls are unknown in this study.

### Stream network food web implications

Patterns of stream metabolism are linked to aquatic food webs, as animals can influence rates of primary and secondary production (e.g., grazing, excretion), and those basal organisms, in turn, provide food for animals. Harshness (as defined by flood intensity, length of dry period, and distance from refugia) has been identified as a strong driver of stream community composition and food web structure (Dodds et al. 2004; Fritz and Dodds 2005). The processes underlying this driving force may include shifts in food sources. We have demonstrated disparate responses of autotrophic and heterotrophic basal organisms to flow return which could have important consequences for local consumers. For example, our data suggest that autotrophic activity slowly increased over time at most sites which should favor, or at least support, grazers in the system. The central stoneroller (*Campostoma anomalum*) and Southern redbelly dace (*Chrosomus erythrogaster*) are dominant species of the stream icthyofauna, are herbivorous, and are highly mobile (Hedden and Gido 2020). During drought, these fishes are concentrated in the few remaining downstream pools, but able to move from these refugia up through the stream network within days once flow returns. Other research in this stream network has shown that fishes may further stimulate metabolic processes (Murdock et al. 2010; Trentman et al. 2020) and alter biofilm microbial biomass accrual and composition (Veach et al. 2018). Our data suggest that ample autochthonous resources should be available to support the upper food web soon after flooding in most reaches of the stream network, contributing in part to the apparent resilience of the animal communities in this harsh habitat.

## Conclusion

This study expands our understanding of stream metabolism and ecosystem function in two ways. First, until recently, most research on stream metabolism consists of relatively short periods of measurement (one or a few days) under baseflow conditions at a single location in a stream or river. While there are continuous estimates of metabolism for single locations in rivers and streams (Uehlinger 2006; Roberts et al. 2007; Reisinger et al. 2017; Bernhardt et al. 2018; Qasem et al. 2019), the deployment of multiple stations within a single watershed following a flood is less common, especially for extended periods. Our study design allowed for determination of flood recovery in a watershed context, to showcase that flood recovery trends can vary greatly within different reaches of a stream network, in relation to antecedent flow conditions, and based on the metric of consideration. Second, our results emphasize the importance of antecedent flow conditions for stream metabolism responses to scouring floods and highlight another effect of increasing intermittency in streams. We show that ER and NEP after flooding can be higher and more heterotrophic, respectively, likely due to differences in physiological responses to water availability and pulses of organic materials between autotrophic and heterotrophic microbes. Such differences have ecosystem-scale implications for the availability of basal resources and energy budgets postflooding. Overall, the results from our study could be particularly important given that future changes in climate may lead to more intense cycles of drought and rewetting in intermittent streams, and to more intermittent streams globally.

## Data availability statement

All raw and processed metabolism and environmental data are available upon request.

## References

Acuna, V., A. Giorgi, I. Munoz, U. Uehlinger, and S. Sabater. 2004. Flow extremes and benthic organic matter shape the metabolism of a headwater Mediterranean stream. Freshw. Biol. **49**: 960–971. doi:10.1111/j.1365-2427.2004.01239.x

Allen, D. C., and others. 2020. River ecosystem conceptual models and non-perennial rivers: A critical review. WIREs Water **7**. doi:10.1002/wat2.1473

Appling, A. P., R. O. Hall, C. B. Yackulic, and M. Arroita. 2018. Overcoming equifinality: Leveraging long time series for stream metabolism estimation. J. Geophys. Res. Biogeo. **123**: 624–645. doi:10.1002/2017JG004140

Barton, K. 2009. Mu-MIn: Multi-model inference. R package version 0.12.2/r18. Available from: http://R-Forge.R-project.org/projects/mumin/

Bates, D., M. Mächler, B. Bolker, and S. Walker. 2015. Fitting linear mixed-effects models using lme4. J. Stat. Softw. **67**: 1–50. doi:10.18637/jss.v067.i01

Battin, T. J., K. Besemer, M. M. Bengtsson, A. M. Romani, and A. I. Packmann. 2016. The ecology and biogeochemistry of stream biofilms. Nat. Rev. Microbiol. **14**: 251–263. doi:10.1038/nrmicro.2016.15

Bernal, S., A. Lupon, W. M. Wollheim, F. Sabater, S. Poblador, and E. Martí. 2019. Supply, demand, and in-stream retention of dissolved organic carbon and nitrate during storms in Mediterranean forested headwater streams. Front. Environ. Sci. **7**: 60. doi:10.3389/fenvs.2019.00060

Bernhardt, E. S., and others. 2018. The metabolic regimes of flowing waters: Metabolic regimes. Limnol. Oceanogr. **63**: S99–S118. doi:10.1002/lno.10726

Bernot, M. J., and others. 2010. Inter-regional comparison of land-use effects on stream metabolism: Inter-regional stream metabolism. Freshw. Biol. **55**: 1874–1890. doi:10.1111/j.1365-2427.2010.02422.x

Besemer, K., G. Singer, R. Limberger, A.-K. Chlup, G. Hochedlinger, I. Hödl, C. Baranyi, and T. J. Battin. 2007. Biophysical controls on community succession in stream biofilms. Appl. Environ. Microbiol. **73**: 4966–4974. doi:10.1128/AEM.00588-07

Cook, R. A., B. Gawne, R. Petrie, D. S. Baldwin, G. N. Rees, D. L. Nielsen, and N. S. P. Ning. 2015. River metabolism and carbon dynamics in response to flooding in a lowland river. Mar. Freshw. Res. **66**: 919. doi:10.1071/MF14199

Corti, R., and T. Datry. 2012. Invertebrates and sestonic matter in an advancing wetted front travelling down a dry river bed (Albarine, France). Freshw. Sci. **31**: 1187–1201. doi:10.1899/12-017.1

Costigan, K. H., M. D. Daniels, and W. K. Dodds. 2015. Fundamental spatial and temporal disconnections in the hydrology of an intermittent prairie headwater network. J. Hydrol. **522**: 305–316. doi:10.1016/j.jhydrol.2014.12.031

Demars, B. O. L. 2019. Hydrological pulses and burning of dissolved organic carbon by stream respiration: Hydrological pulses and stream respiration. Limnol. Oceanogr. **64**: 406–421. doi:10.1002/lno.11048

Demars, B. O. L., and others. 2011. Temperature and the metabolic balance of streams: Temperature and the metabolic balance of streams. Freshw. Biol. **56**: 1106–1121. doi:10.1111/j.1365-2427.2010.02554.x

Dodds, W. 2020*a*. ASD06 Stream discharge measured at the flumes on watershed N02B at Konza Prairie ver 11. Environmental Data Initiative. [Accessed 2020 July 13]. https://doi.org/10.6073/pasta/0d90c63700f164241074d1f5835c43cb

Dodds, W. 2020*b*. ASD05 Stream discharge measured at the flumes on watershed N01B at Konza Prairie ver 12. Environmental Data Initiative. [Accessed 2020 July 13]. https://doi.org/10.6073/pasta/5794ee6297c6cabca6169aa2c7cf082c

Dodds, W. 2020*c*. ASD04 Stream discharge measured at the flumes on watershed N20B at Konza Prairie ver 11. Environmental Data Initiative. [Accessed 2020 July 13]. https://doi.org/10.6073/pasta/03fa19934fafebe716f3bfd791a4d3d9

Dodds, W. 2020*d*. ASD02 Stream discharge measured at the flumes on watershed N04D at Konza Prairie ver 11. Environmental Data Initiative. [Accessed 2020 July 13]. https://doi.org/10.6073/pasta/1fb12b7396226b8cb6f785140be36c4c

Dodds, W. K., R. E. Hutson, A. C. Eichem, M. A. Evans, D. A. Gudder, K. M. Fritz, and L. Gray. 1996. The relationship of floods, drying, flow and light to primary production and producer biomass in a prairie stream. Hydrobiologia **333**: 151–159. doi:10.1007/BF00013429

Dodds, W. K., K. Gido, M. R. Whiles, K. M. Fritz, and W. J. Matthews. 2004. Life on the edge: The ecology of Great Plains Prairie streams. Bioscience **54**: 205. doi:10.1641/0006-3568(2004)054[0205:LOTETE]2.0.CO;2

Dodds, W. K., K. Gido, M. R. Whiles, M. D. Daniels, and B. P. Grudzinski. 2015. The stream biome gradient concept: Factors controlling lotic systems across broad biogeographic scales. Freshw. Sci. **34**: 1–19. doi:10.1086/679756

Farrell, K. J., and others. 2018. Variation in detrital resource stoichiometry signals differential carbon to nutrient limitation for stream consumers across biomes. Ecosystems **21**: 1676–1691. doi:10.1007/s10021-018-0247-z

Fierer, N., and J. P. Schimel. 2002. Effects of drying–rewetting frequency on soil carbon and nitrogen transformations. Soil Biol. Biochem. **34**(6): 777–787

Fisher, S. G., L. J. Gray, N. B. Grimm, and D. E. Busch. 1982. Temporal succession in a desert stream ecosystem following flash flooding. Ecol. Monogr. **52**: 93–110. doi:10.2307/2937346

Francoeur, S. N., and B. J. F. Biggs. 2006. Short-term effects of elevated velocity and sediment abrasion on benthic algal communities. Hydrobiologia **561**: 59–69. doi:10.1007/s10750-005-1604-4

Fritz, K. M., and W. K. Dodds. 2005. Harshness: Characterisation of intermittent stream habitat over space and time. Mar. Freshw. Res. **56**: 13. doi:10.1071/MF04244

Frost, P. C., C. T. Cherrier, J. H. Larson, S. Bridgham, and G. A. Lamberti. 2007. Effects of dissolved organic matter and ultraviolet radiation on the accrual, stoichiometry and algal taxonomy of stream periphyton. Freshw. Biol. **52**: 319–330. doi:10.1111/j.1365-2427.2006.01696.x

Grace, M. R., D. P. Giling, S. Hladyz, V. Caron, R. M. Thompson, and R. Mac Nally. 2015. Fast processing of diel oxygen curves: Estimating stream metabolism with BASE (BAyesian Single-station Estimation): Fast processing of diel oxygen curves. Limnol. Oceanogr. Methods **13**: e10011. doi:10.1002/lom3.10011

Grimm, N. B. 1987. Nitrogen dynamics during succession in a desert stream. Ecology **68**: 1157–1170. doi:10.2307/1939200

Gudmundsson, L., J. Boulange, H. X. Do, S. N. Gosling, M. G. Grillakis, A. G. Koutroulis, M. Leonard, J. Liu, H. Müller Schmied, L. Papadimitriou, and Y. Pokhrel. 2021. Globally observed trends in mean and extreme river flow attributed to climate change. Science **371**(6534): 1159–1162.

Hayden, B. 1998. Regional climate and the distribution of tallgrass prairie, p. 19–34. *In* Grassland dynamics: Long-term ecological research in tallgrass prairie. Oxford Univ. Press.

Hedden, S. C., and K. B. Gido. 2020. Dispersal drives changes in fish community abundance in intermittent stream networks. River Res. Appl. **36**: 797–806. doi:10.1002/rra.3599

Jones, J. B., S. G. Fisher, and N. B. Grimm. 1995. Vertical hydrologic exchange and ecosystem metabolism in a Sonoran Desert stream. Ecology **76**: 942–952. doi:10.2307/1939358

Kosinski, R. J. 1984. A comparison of the accuracy and precision of several open-water oxygen productivity techniques. Hydrobiologia **119**: 139–148. doi:10.1007/BF00011953

Larned, S. T., T. Datry, D. B. Arscott, and K. Tockner. 2010. Emerging concepts in temporary-river ecology. Freshw. Biol. **55**: 717–738. doi:10.1111/j.1365-2427.2009.02322.x

Larson, D. M., W. K. Dodds, and A. M. Veach. 2019. Removal of woody Riparian vegetation substantially altered a stream ecosystem in an otherwise undisturbed grassland watershed. Ecosystems **22**: 64–76. doi:10.1007/s10021-018-0252-2

Leigh, C., A. J. Boulton, J. L. Courtwright, K. Fritz, C. L. May, R. H. Walker, and T. Datry. 2016. Ecological research and management of intermittent rivers: An historical review and future directions. Freshw. Biol. **61**: 1181–1199. doi:10.1111/fwb.12646

Lennon, J. T., and S. E. Jones. 2011. Microbial seed banks: The ecological and evolutionary implications of dormancy. Nat. Rev. Microbiol. **9**: 119–130. doi:10.1038/nrmicro2504

Matthews, W. J. 1988. North American Prairie streams as systems for ecological study. J. North Am. Benthol. Soc. **7**: 387–409. doi:10.2307/1467298

McKew, B. A., J. D. Taylor, T. J. McGenity, and G. J. C. Underwood. 2011. Resistance and resilience of benthic biofilm communities from a temperate saltmarsh to desiccation and rewetting. ISME J. **5**: 30–41. doi:10.1038/ismej.2010.91

Mejia, F. H., A. K. Fremier, J. R. Benjamin, J. R. Bellmore, A. Z. Grimm, G. A. Watson, and M. Newsom. 2019. Stream metabolism increases with drainage area and peaks asynchronously across a stream network. Aquat. Sci. **81**: 1–17. doi:10.1007/s00027-018-0606-z

Messager, M. L., B. Lehner, C. Cockburn, N. Lamouroux, H. Pella, T. Snelder, K. Tockner, T. Trautmann, C. Watt, and T. Datry 2021. Global prevalence of non-perennial rivers and streams. Nature **594**(7863): 391–397.

Mulholland, P. J., and others. 2001. Inter-biome comparison of factors controlling stream metabolism. Freshw. Biol. **46**: 1503–1517. doi:10.1046/j.1365-2427.2001.00773.x

Murdock, J. N., K. B. Gido, W. K. Dodds, K. N. Bertrand, and M. R. Whiles. 2010. Consumer return chronology alters recovery trajectory of stream ecosystem structure and function following drought. Ecology **91**: 1048–1062. doi:10.1890/08-2168.1

Odum, H. T. 1956. Primary production in flowing waters. Limnol. Oceanogr. **1**: 102–117. doi:10.4319/lo.1956.1.2.0102

Palmer, M., and A. Ruhi. 2019. Linkages between flow regime, biota, and ecosystem processes: Implications for river restoration. Science **365**: eaaw2087. doi:10.1126/science.aaw2087

Parkhill, K. L., and J. S. Gulliver. 1999. Modeling the effect of light on whole-stream respiration. Ecol. Model. **117**: 333–342. doi:10.1016/S0304-3800(99)00017-4

Passy, S. I., and C. A. Larson. 2011. Succession in stream biofilms is an environmentally driven gradient of stress tolerance. Microb. Ecol. **62**: 414–424. doi:10.1007/s00248-011-9879-7

Poff, N. L., J. D. Allan, M. Bain, J. R. Karr, K. L. Prestegaard, B. D. Richter, R. Sparks, and J. C. Stromberg. 1997. The natural flow regime: A paradigm for river conservation and restoration. Bioscience **47**: 769–784.

Poff, N. L., and J. K. H. Zimmerman. 2010. Ecological responses to altered flow regimes: A literature review to inform the science and management of environmental flows: Review of altered flow regimes. Freshw. Biol. **55**: 194–205. doi:10.1111/j.1365-2427.2009.02272.x

Qasem, K., S. Vitousek, B. O'Connor, and T. Hoellein. 2019. The effect of floods on ecosystem metabolism in suburban streams. Freshw. Sci. **38**: 412–424. doi:10.1086/703459

Reisinger, A. J., E. J. Rosi, H. A. Bechtold, T. R. Doody, S. S. Kaushal, and P. M. Groffman. 2017. Recovery and resilience of urban stream metabolism following Superstorm Sandy and other floods. Ecosphere **8**. doi:10.1002/ecs2.1776

Riley, A. J., and W. K. Dodds. 2013. Whole-stream metabolism: Strategies for measuring and modeling diel trends of dissolved oxygen. Freshw. Sci. **32**: 56–69. doi:10.1899/12-058.1

Roberts, B. J., P. J. Mulholland, and W. R. Hill. 2007. Multiple scales of temporal variability in ecosystem metabolism

rates: Results from 2 years of continuous monitoring in a forested headwater stream. Ecosystems **10**: 588–606. doi:10.1007/s10021-007-9059-2

Rüegg, J., J. J. Eichmiller, N. Mladenov, and W. K. Dodds. 2015. Dissolved organic carbon concentration and flux in a grassland stream: Spatial and temporal patterns and processes from long-term data. Biogeochemistry **125**: 393–408. doi:10.1007/s10533-015-0134-z

Rüegg, J., and others. 2016. Baseflow physical characteristics differ at multiple spatial scales in stream networks across diverse biomes. Landsc. Ecol. **31**: 119–136. doi:10.1007/s10980-015-0289-y

Sabater, S., X. Timoner, C. Borrego, and V. Acuña. 2016. Stream biofilm responses to flow intermittency: From cells to ecosystems. Front. Environ. Sci. **4**: 14. doi:10.3389/fenvs.2016.00014

Salazar, A., B. N. Sulman, and J. S. Dukes. 2018. Microbial dormancy promotes microbial biomass and respiration across pulses of drying-wetting stress. Soil Biol. Biochem. **116**: 237–244. doi:10.1016/j.soilbio.2017.10.017

Samson, F., and F. Knopf. 1994. Prairie conservation in North America. Bioscience **44**: 418–421. doi:10.2307/1312365

Schechner, A. E., W. K. Dodds, F. Tromboni, S. Chandra, and A. Maasri. 2021. How do methodological choices influence estimation of river metabolism? Limnol. Oceanogr. Methods **19**: 659–672. doi:10.1002/lom3.10451

Schiller, D., and others. 2019. Sediment respiration pulses in intermittent rivers and ephemeral streams. Global Biogeochem. Cycl. **33**: 1251–1263. doi:10.1029/2019GB006276

Schimel, J. P. 2018. Life in dry soils: Effects of drought on soil microbial communities and processes. Annu. Rev. Ecol. Evol. Syst. **49**: 409–432. doi:10.1146/annurev-ecolsys-110617-062614

Seybold, E., and B. McGlynn. 2018. Hydrologic and biogeochemical drivers of dissolved organic carbon and nitrate uptake in a headwater stream network. Biogeochemistry **138**: 23–48. doi:10.1007/s10533-018-0426-1

Song, C., W. K. Dodds, M. T. Trentman, J. Rüegg, and F. Ballantyne. 2016. Methods of approximation influence aquatic ecosystem metabolism estimates: Approximation influences metabolism estimates. Limnol. Oceanogr. Methods **14**: 557–569. doi:10.1002/lom3.10112

Summers, B. M., and others. 2020. Long-term data reveal highly-variable metabolism and transitions in trophic status in a montane stream. Freshwater Science **39**: 241–255. doi:10.1086/708659

Timoner, X., V. Acuña, D. Von Schiller, and S. Sabater. 2012. Functional responses of stream biofilms to flow cessation, desiccation and rewetting: Flow intermittency effects on stream biofilms. Freshw. Biol. **57**: 1565–1578. doi:10.1111/j.1365-2427.2012.02818.x

Tooth, S. 2000. Process, form and change in dryland rivers: A review of recent research. Earth Sci. Rev. **51**: 67–107. doi:10.1016/S0012-8252(00)00014-3

Trentman, M. T., W. K. Dodds, K. B. Gido, J. Rüegg, and C. M. Ruffing. 2020. Using path analysis to determine interacting effects of biotic and abiotic factors on patch-scale biogeochemical rates in a prairie stream. Aquat. Sci. **82**: 1–11. doi:10.1007/s00027-020-0702-8

Uehlinger, U. 2000. Resistance and resilience of ecosystem metabolism in a flood-prone river system. Freshw. Biol. **45**: 319–332. doi:10.1111/j.1365-2427.2000.00620.x

Uehlinger, U. 2006. Annual cycle and inter-annual variability of gross primary production and ecosystem respiration in a floodprone river during a 15-year period. Freshw. Biol. **51**: 938–950. doi:10.1111/j.1365-2427.2006.01551.x

Uehlinger, U., and M. W. Naegeli. 1998. Ecosystem metabolism, disturbance, and stability in a Prealpine gravel bed river. J. North Am. Benthol. Soc. **17**: 165–178. doi:10.2307/1467960

Valett, H. M., C. L. Crenshaw, and P. F. Wagner. 2002. Stream nutrient uptake, forest succession, and biogeochemical theory. Ecology **83**(10): 2888–2901

Veach, A. M., W. K. Dodds, and A. Skibbe. 2014. Fire and grazing influences on rates of Riparian woody plant expansion along grassland streams. PLoS One **9**: e106922. doi:10.1371/journal.pone.0106922

Veach, A. M., J. C. Stegen, S. P. Brown, W. K. Dodds, and A. Jumpponen. 2016. Spatial and successional dynamics of microbial biofilm communities in a grassland stream ecosystem. Mol. Ecol. **25**: 4674–4688. doi:10.1111/mec.13784

Veach, A. M., M. J. Troia, A. Jumpponen, and W. K. Dodds. 2018. Top–down effects of a grazing, omnivorous minnow (*Campostoma anomalum*) on stream microbial communities. Freshw. Sci. **37**: 121–133. doi:10.1086/696292

Vitousek, P. M., and W. A. Reiners. 1975. Ecosystem succession and nutrient retention: A hypothesis. Bioscience **25**: 376–381. doi:10.2307/1297148

Wohl, E., R. O. Hall, K. B. Lininger, N. A. Sutfin, and D. M. Walters. 2017. Carbon dynamics of river corridors and the effects of human alterations. Ecol. Monogr. **87**: 379–409. doi:10.1002/ecm.1261

Yates, A. G., R. B. Brua, J. M. Culp, R. G. Young, and P. A. Chambers. 2018. Variation in stream metabolism and benthic invertebrate composition along longitudinal profiles of two contrasting river systems. Can. J. Fish. Aquat. Sci. **75**: 549–559. doi:10.1139/cjfas-2016-0198

Young, R. G., C. D. Matthaei, and C. R. Townsend. 2008. Organic matter breakdown and ecosystem metabolism: Functional indicators for assessing river ecosystem health. J. North Am. Benthol. Soc. **27**: 605–625. doi:10.1899/07-121.1

Zeglin, L. H., and others. 2013. Altered precipitation regime affects the function and composition of soil microbial communities on multiple time scales. Ecology **94**: 2334–2345. doi:10.1890/12-2018.1

Zuur, A. F., E. N. Ieno, N. J. Walker, A. A. Saveliev, and G. M. Smith. 2009. Mixed effects modelling for nested data, p. 101–142. *In* Mixed effects models and extensions in ecology with R. Springer.

## Conflict of Interest

The authors declare no conflicts related to this work.